

POWER MANAGEMENT OF MULTI-PORT ISOLATED DC-DC CONVERTER FOR PHOTOVOLTAIC APPLICATIONS

Samuel Raj¹, S. Gopal Reddy²

¹ Student, EEE Department, Jyothismathi Institute of technology & Science, Telangana, India

² Assoc.Prof, EEE Department, Jyothismathi Institute of technology & Science, Telangana, India

ABSTRACT

This paper proposes an isolated multiport dc-dc converter for simultaneous power management of multiple renewable energy sources, which can be of different types and capacities. The proposed dc-dc converter only uses one controllable switch in each port to which a source is connected. Therefore, it has the advantages of simple topology and minimum number of power switches. A general topology of the proposed converter is first introduced. Its principle and operation are then analyzed. The proposed converter is applied for simultaneous maximum power point tracking (MPPT) control of a solar power generation systems consisting of multiple different photovoltaic (PV) panels. The simulation results are provided to validate the effectiveness of using the proposed converter to achieve MPPT simultaneously for the all PV panels.

Keyword: -DC-DC Converter, maximum power point tracking (MPPT), multiport converter

1. INTRODUCTION

Now a days there is a growing interest in generating electricity from distributed renewable energy sources. In many applications, it is required to connect multiple renewable energy sources of different types (e.g., wind and solar) and capacities to a power grid or load [1]–[6]. To perform efficient power management and grid integration for the multiple sources, multiport dc-dc converters have been proposed [5]–[10]. Fig. 3 shows a two-stage, grid-connected multi source renewable energy system, which consists of an isolated multiport dc-dc converter and an inverter [11]. The isolated dc-dc converter has multiple input ports for connecting different sources, such as photovoltaic (PV) panels, wind turbine generators (WTGs), fuel cells, and so on. The multiport dc-dc converter not only regulates the low-level dc voltages of the sources to a constant high level required by the inverter, but also can provide other important control functions, such as maximum power point tracking (MPPT), for the renewable energy sources.

There are two categories of integrated isolated multiport converters. One category of converters uses a transformer with a separate winding for each port. Therefore, all ports are electrically isolated [12]–[17]. The other category of converters has multiple ports connected to a single winding on the primary side of a transformer [18]–[25], as shown in Fig. 1. It requires a common ground point for all the input sources. The second topology is preferable due to the advantage of using less number of windings in the transformer. A number of isolated multiport converters belonging to the second category have been proposed. A widely used topology is the isolated half-bridge converter [7], which used $2m + 2$ controllable switches, where $m(m \geq 2)$ is the number of input ports. Thereafter, in this paper, controllable switches are also called switches. The number of switches was reduced to $2m$ by either using one source as the dc link [21], [22] or reducing switches on the secondary side of the transformer [25]. Recently, a multiport converter topology with $m + 3$ power switches has been proposed [5]. When $m > 3$, this multiport converter has the least number of switches among the existing topologies.

This paper proposes a new isolated multiport dc-dc converter for simultaneous power management of multiple renewable energy sources [26], where only one switch is used in each input port connected to a source. Similar to the converter in [25], the proposed converter does not use any controllable switch on the secondary side of the

transformer. Compared with the existing multiport dc–dc converter topologies [18]–[25], the proposed converter has the least number of switches and thereby a lower cost.

2 SOFT SWITCHING TECHNIQUES

A soft switching technique refers to the both zero voltage switching and zeros current switching. The making or breaking of circuit timed such that the transition occurs when the voltage wave form crosses zero voltage is known as the Zero voltage switching. Quasi-resonant switching is a good technique for improving voltage-converter efficiency, but things can be further improved by implementing full soft switching. During soft switching the voltage falls to zero (rather than just a minimum) before the MOSFET is turned on or off, eliminating any overlap between voltage and current and minimizing losses. (The technique can also be used to switch the MOSFET when current, rather than voltage, reaches zero. This is known as Zero Current Switching (ZCS).) An additional advantage is that the smooth switching waveforms minimize EMI Soft switching (ZVS) can best be defined as conventional PWM power conversion during the MOSFET’s on-time but with “resonant” switching transitions.

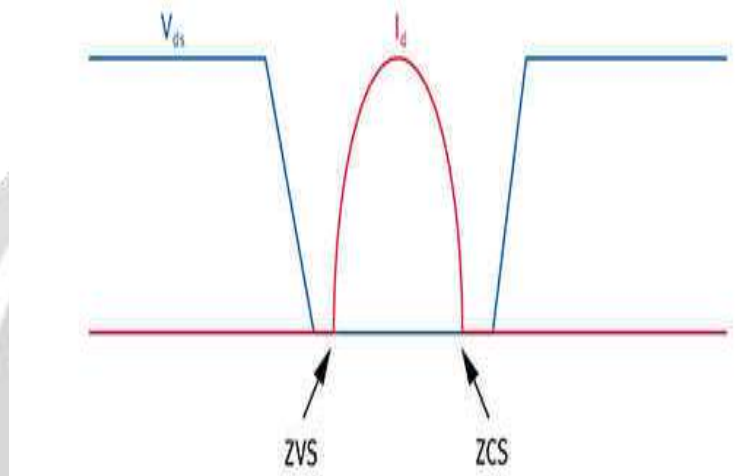


Fig-1: switching techniques

The technique can be considered PWM power utilizing a constant off-time control which varies the conversion frequency, or on-time to maintain regulation of the output voltage. For a given unit of time, this method is similar to fixed-frequency conversion using an adjustable duty cycle. Regulation of the output voltage is achieved by adjusting the effective duty cycle (and thus on-time), by varying the conversion frequency. During the ZVS switch off-time, the regulator’s L-C circuit resonates traversing the voltage across the switch from zero to its peak and back down again to zero when the switch can be reactivated, and lossless ZVS facilitated. The MOSFET transition losses are zero—regardless of operating frequency and input voltage—representing a significant savings in power, and a substantial improvement in efficiency (Figure 5). Such attributes make ZVS a good technique for high-frequency, high-voltage converter designs.

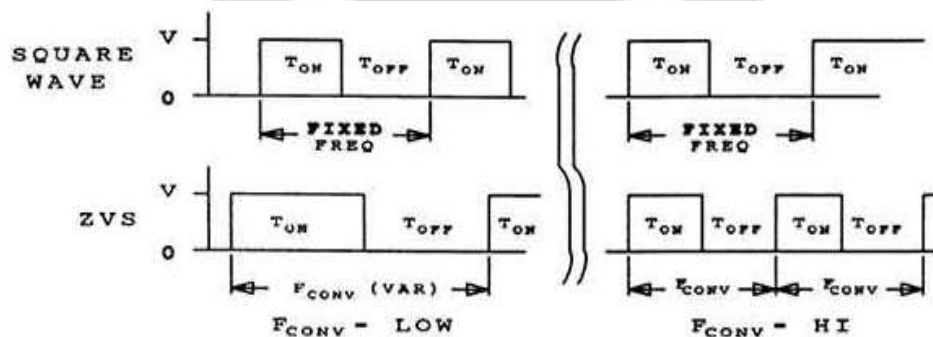


Fig-2: conventional pwm waveforms

The above figure shows the Conventional PWM employs a fixed frequency, but varies the duty cycle to achieve regulation; in contrast, ZVS varies the conversion frequency (which in turn alters the on-time) to maintain output

voltage. Two other advantages of ZVS are that it reduces the harmonic spectrum of any EMI (centering it on the switching frequency) and allows higher frequency operation resulting in reduced, easier-to-filter noise and the use of smaller filter components.

3. PROPOSED SYSTEM

A new isolated multiport dc–dc converter for simultaneous power management of multiple renewable energy sources [26], where only one switch is used in each input port connected to a source. Similar to the converter in [25], the proposed converter does not use any controllable switch on the secondary side of the transformer. Compared with the existing multiport dc–dc converter topologies [18]–[25], the proposed converter has the least number of switches and thereby a lower cost. The proposed converter is applied for power management of a wind/solar hybrid generation system, which consists of a WTG and two different PV panels. Using a suitably designed perturbation and observation (P&O) MPPT algorithm, the WTG and PV panels can be controlled simultaneously to extract the maximum power from wind and sunlight, respectively, using the proposed converter.

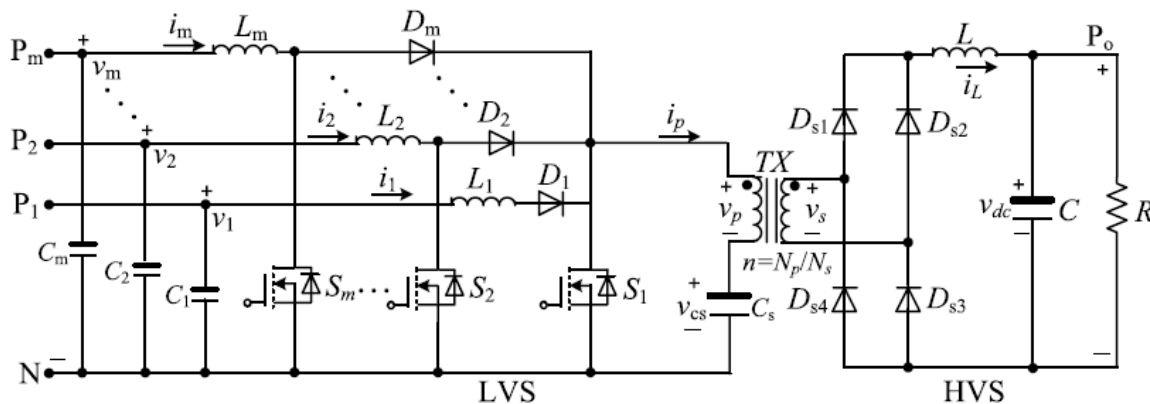
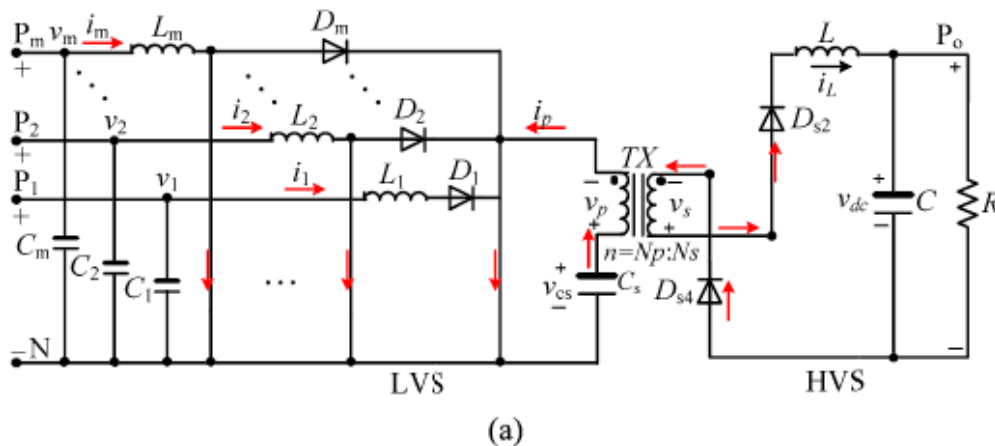


Fig-3: Topology of the proposed isolated multiport dc–dc converter.

Fig. 3 shows the circuit diagram of the proposed isolated multiport dc–dc converter. It consists of a low-voltage side (LVS) circuit and a high-voltage-side (HVS) circuit connected by a high-frequency transformer TX. The LVS circuit consists of m ports in parallel, one energy storage capacitor C_s , and the primary winding of the transformer. Each port contains a controllable power switch, a power diode, and an inductor. The HVS circuit consists of the secondary winding of the transformer connected to a full-bridge diode rectifier, and a low-frequency LC filter. The transformer’s turn ratio is defined as $n = N_p / N_s$, where N_p and N_s are the numbers of turns of the primary and secondary windings, respectively.

This converter has three operating modes: 1) all switches are on; 2) switch S_1 is off while at least one of the other switches is on; and 3) all switches are off. The equivalent circuits of the converter in the three operating modes are shown in Fig. 4.



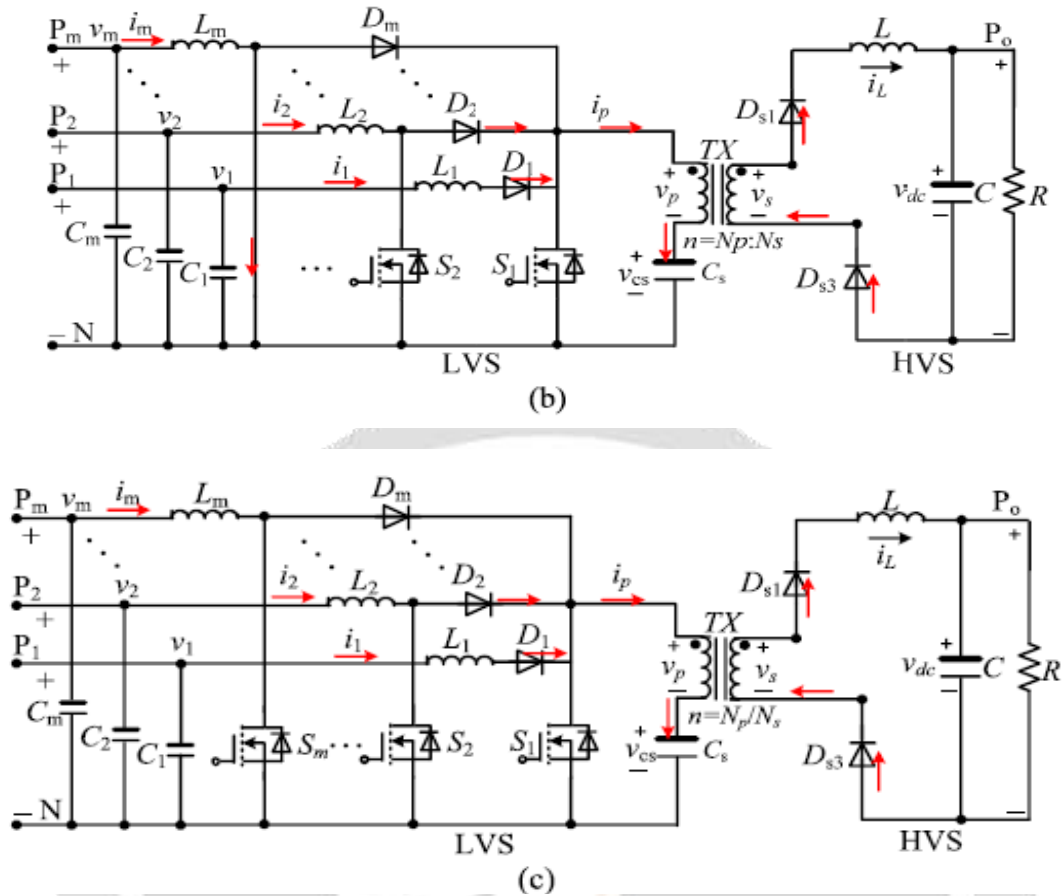


Fig-4: Equivalent circuits of the three operating modes of the proposed converter. (a) Mode 1: all switches are on. (b) Mode 2: S_1 is off and at least one of the other switches is on. (c) Mode 3: all switches are off.

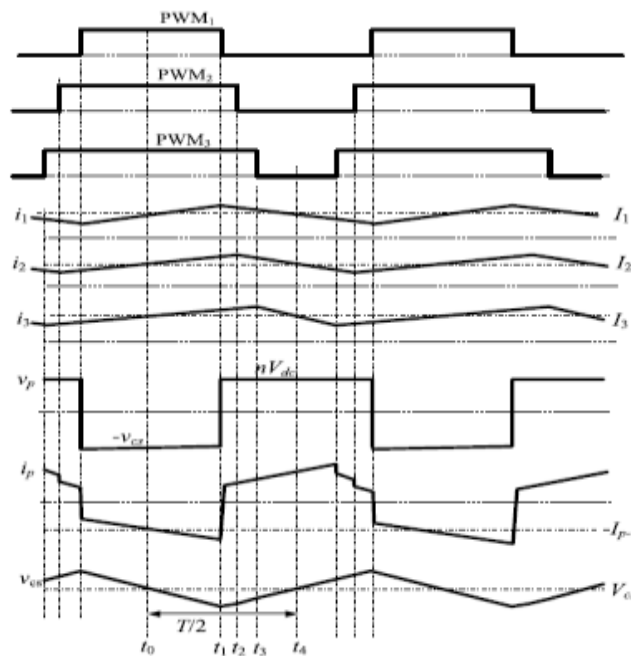


Fig-5: Waveforms of the proposed converter when $m = 3$.

Fig. 5 shows the steady-state waveforms of the converter in one switching period covering the three operating modes when $m = 3$. To facilitate the explanation of the converter operation, the state-space equations for different modes.

TABLE-1: Component specifications of the converter

L_1	420 μH	$C_1 \sim C_3$	1000 μF
L_2	280 μH	C_5	1000 μF
L_3	300 μH	C	1000 μF
L	1120 μH	n	7:28
S_1	FDP24N40	$S_2 \sim S_3$	FDP3632
$D_1 \sim D_3$	MUR1510	$DS_1 \sim DS_4$	EGP50D

4 SIMULATION RESULTS

Fig. 8(a) shows the measured waveforms of the currents i_1 and i_2 flowing through the two inductors L_1 and L_2 , respectively, where i_1 and i_2 increase when the two switches S_1 and S_2 are switched on; when the two switches are off, i_1 and i_2 decrease.

Fig. 8(b) shows the current waveforms of the two inductors L_2 and L_3 , where i_3 is the current flowing through the inductor L_3 . i_3 increases when the switch S_3 is switched on and decreases when S_3 is off, which is similar to i_1 and i_2 . The mean values of the three source currents in Fig. 8(a) and (b) are $I_1 = 1.41 \text{ A}$, $I_2 = 3.82 \text{ A}$, and $I_3 = 3.28 \text{ A}$, which shows that the three sources WTG, PV1, and PV2 are connected to the multiport dc–dc converter to supply power simultaneously.

Fig. 8(c) shows the waveform of i_p , which is the current flowing through the primary side of the transformer. When S_1 is on, the capacitor C_s discharges since the current is negative; during the period when S_1 is off, the current becomes positive, which charges C_s ; when S_2 is off, i_p increases because $i_p = i_1+i_2$; i_p further increases to $i_1+i_2+i_3$ when all of the three switches are off. The waveforms in Fig. 8 are consistent with those in Fig. 4, which validates the theoretical analysis.

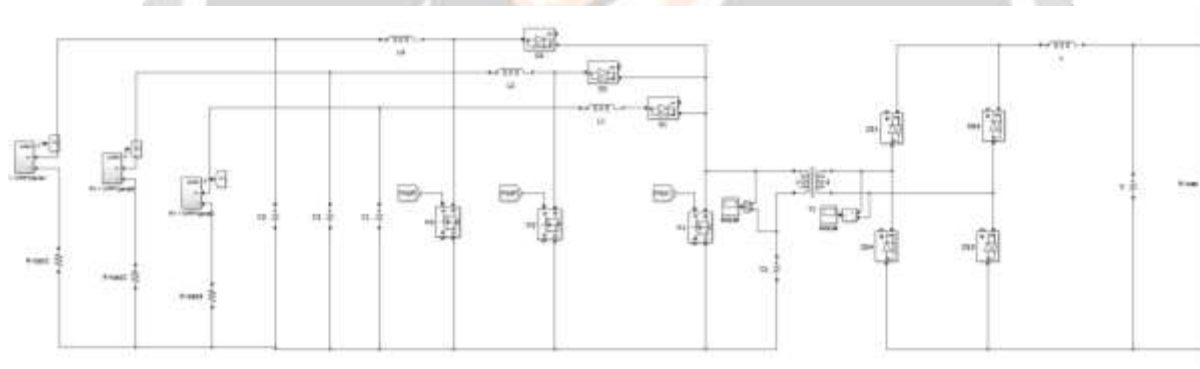


Fig-6: Simulation circuit of the proposed converter with different rating solar panels

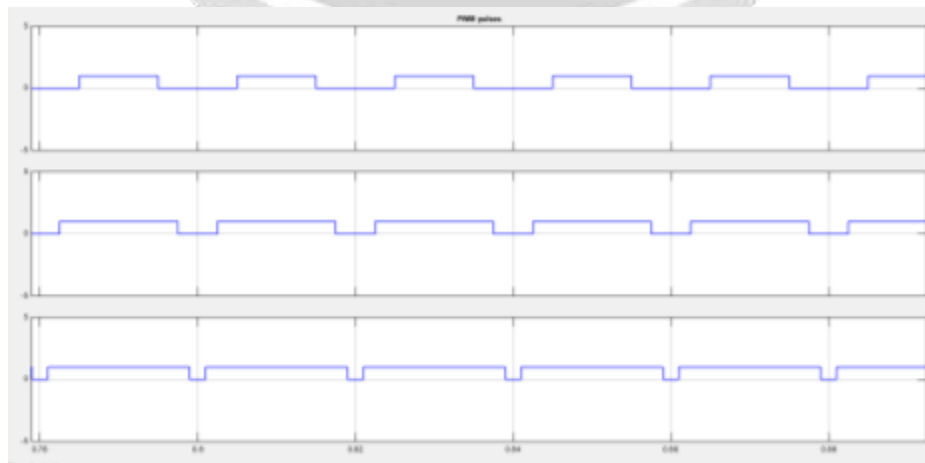


Fig-7: pwm pulses for the MOSFETs waveforms

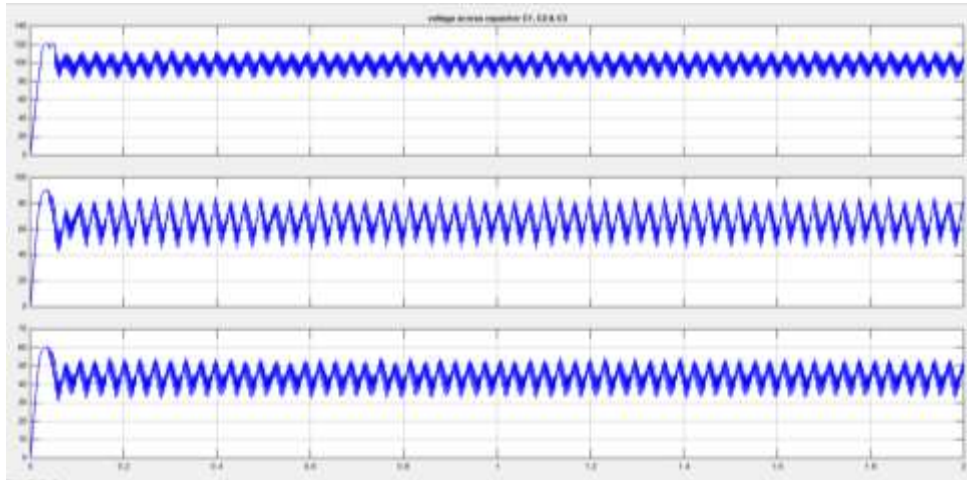


Fig-8: voltage across capacitors c_1 , c_2 and c_3 waveforms

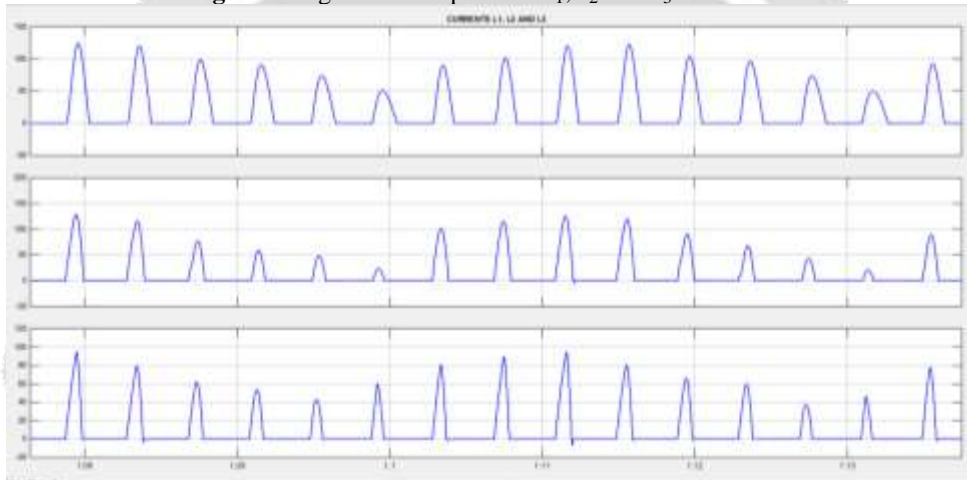


Fig-9: current through L_1 , L_2 and L_3 waveforms

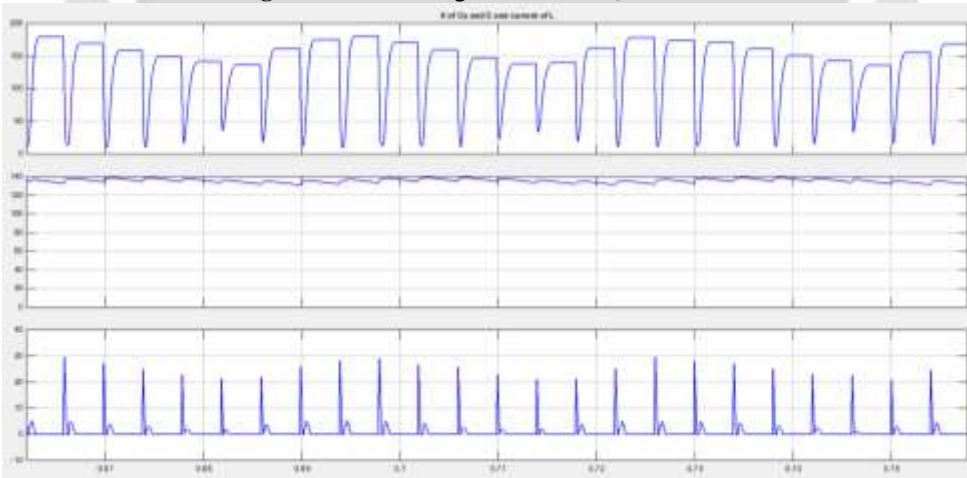


Fig-10: voltage across capacitors c_s , c and current through L waveforms

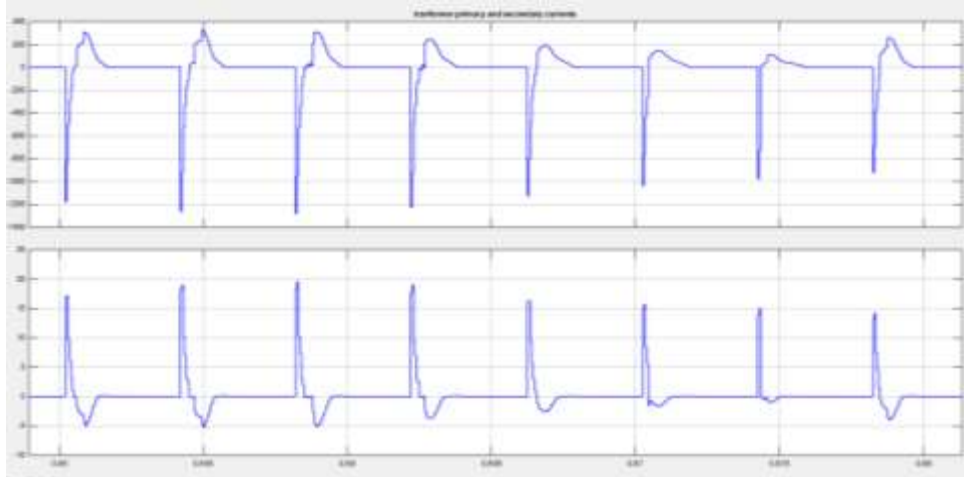


Fig-11: transformer primary and secondary currents waveforms

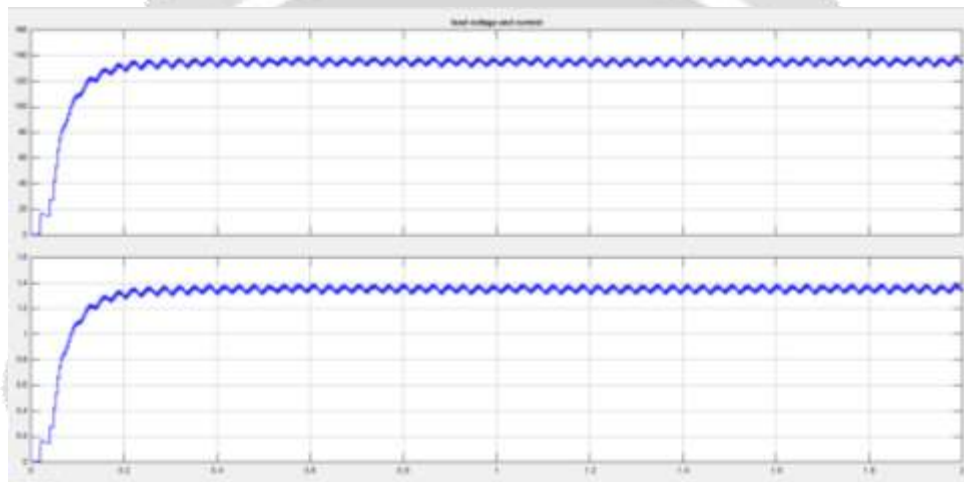


Fig-12: load voltage and current waveforms

5. CONCLUSIONS

An isolated multiport dc–dc converter that uses the minimum number of switches has been proposed for simultaneous power management of multiple renewable energy sources. The proposed converter has been applied for simultaneous power management of a three-source wind/solar hybrid generation system. The simulation results have been provided to show the effectiveness of the proposed converter using MATLAB. The advantage of the proposed multiport dc–dc converter is its simple topology while having the capability of MPPT control for different renewable energy sources simultaneously. Moreover, the proposed converter can be easily applied for power management of other types of renewable energy sources.

6. REFERENCES

- [1] J. Kassakian and T. Jahns, “Evolving and emerging applications of power electronics in systems,” *IEEE J. Emerging Sel. Topics Power Electron.*, vol. 1, no. 2, pp. 47–58, Jun. 2013.
- [2] O. Lucia, I. Cvetkovic, H. Samago, D. Boroyevich, P. Mattavelli, and F. C. Lee, “Design of home appliances for a DC-based nanogrid system: An induction range study case,” *IEEE J. Emerging Sel. Topics Power Electron.*, vol. 1, no. 4, pp. 315–326, Dec. 2013.
- [3] J. Carr, J. Balda, and A. Mantooth, “A high frequency link multiport converter utility interface for renewable energy resources with integrated energy storage,” in *Proc. IEEE Energy Convers. Congr. Exposit.*, Sep. 2010, pp. 3541–3548.
- [4] M. Mahdavi and H. Farzanehfard, “Bridgeless SEPIC PFC rectifier with reduced components and conduction losses,” *IEEE Trans. Ind. Electron.*, vol. 58, no. 9, pp. 4153–4160, Sep. 2011.

- [5] A. A. Fardoun, E. H. Ismail, A. J. Sabzali, and M. A. Al-Saffar, "New efficient bridgeless Cuk rectifiers for PFC applications," *IEEE Trans. Power Electron.*, vol. 27, no. 7, pp. 3292–3301, Jul. 2012.
- [6] E. H. Ismail, "Bridgeless SEPIC rectifier with unity power factor and reduced conduction losses," *IEEE Trans. Ind. Electron.*, vol. 56, no. 4, pp. 1147–1157, Apr. 2009.
- [7] B. Su, J. Zhang, and Z. Lu, "Totem-pole boost bridgeless pfc rectifier with simple zero-current detection and full-range zvs operating at the boundary of DCM/CCM," *IEEE Trans. Power Electron.*, vol. 26, no. 2, pp. 427–435, Feb. 2011.
- [8] J. Zhang, B. Su, and Z. Lu, "Single inductor three-level bridgeless boost power factor correction rectifier with nature voltage clamp," *IET Power Electron.*, vol. 5, no. 3, pp. 358–365, Mar. 2012.
- [9] Y. Cho and J.-S. Lai, "Digital plug-in repetitive controller for single-phase bridgeless pfc converters," *IEEE Trans. Power Electron.*, vol. 28, no. 1, pp. 165–175, Jan. 2013.
- [10] A. A. Fardoun, E. H. Ismail, A. J. Sabzali, and M. A. Al-Saffar, "Bridgeless resonant pseudo boost PFC rectifier," *IEEE Trans. Power Electron.*, vol. 29, no. 11, pp. 5949–5960, Nov. 2014.
- [11] R. Gules, W. M. Santos, F. A. Reis, E. F. R. Romaneli, and A. A. Badin, "A modified SEPIC converter with high static gain for renewable applications," *IEEE Trans. Power Electron.*, vol. 29, no. 11, pp. 5860–5871, Nov. 2014.
- [12] P. F. de Melo, R. Gules, E. F. R. Romaneli, and R. C. Annunziato, "A modified SEPIC converter for high-power-factor rectifier and universal input voltage applications," *IEEE Trans. Power Electron.*, vol. 25, no. 2, pp. 310–321, Feb. 2010.

